GLINT

February 1999

Prepared by:

Schafer Corporation
2000 Randolph Rd. S. E.
Suite 205
Albuquerque, NM 87106

Task Report - Naval Research Laboratory
Contract N00014-97-D-2014/001

SCHAFER CORPORATION

GLINT

February 1999

Prepared by:

Schafer Corporation
2000 Randolph Rd. S. E.
Suite 205
Albuquerque, NM 87106

Task Report - Naval Research Laboratory
Contract N00014-97-D-2014/001

GLINT

Introduction

GLINT is the acronym for Geo Light Imaging National Testbed. Schafer has supported this AFRL program in three basic areas for the Surveillance Technologies Branch (DEBS). The first area is the collation of information to develop a target database of geosynchronous (GEO) satellites. Each possible target needs to be investigated in order to obtain permission from the owner/operator to illuminate it. This information, when obtained, would be part of the database as well. The second area addresses a major operational concern for GLINT. A necessary prerequisite to illumination of GEO satellites by GLINT is the ability to ascertain that the object acquired is the intended target. The GEO satellites are unresolved to any single pupil associated with aperture sizes we are now capable of building. GLINT will be able to image them using an active Fourier telescopy scheme. However, due to international agreements and the safety of instrumentation on-board these satellites, a non-imaging method to first identify that the acquired object is the target in question. This second area is the Signatures Program. Its goal is to pursue non-imaging techniques to obtain satellite information and reduce uncertain identification (ID) in preparation for active illumination by GLINT. The final area of support was the study on a relay mirror experiment that could be performed with GLINT.

GLINT Target Database

A database was created to enable target selection for the passive experiments and also for passive ID prior to active illumination by GLINT. Information on the satellite systems was included to aide the passive identification process. The database now contains the following information: catalog number, satellite name, bus structure, status, orbital inclination, eccentricity, orbit type, longitude (if applicable), number of revolutions per day, country, and a description field. The database also contains information on whether the satellite can be seen from New Mexico or Maui, and if it has been illuminated. Finally, the database contains a table of estimated magnitudes which provide an indication of the range in brightness that the satellite would have when observed. A sample view of the database is shown in Figure 1.

Schafer also supported the GLINT science team. The preliminary GEO database that was created for the passive effort was presented to some other members of the science team. Search capabilities were added to the database as shown in Figure 2.

Briefings were prepared for the GLINT Technical Interchange Meeting (TIM) with the GLINT contractors and science team to present information on the target database. Schafer presented a summary of the target selection database development at the TIM in Socorro, NM on 4 November 1998 (Attch 1).

Signatures Program

Schafer supported the passive identification aspect of GLINT in the Signatures Program. Simulations were performed to tie radiometry simulation results to observations that were made at Capilla Peak Observatory of GEO satellites. The results with TASAT 6.0 were below expectations as seen in Figure 3. At the time of this final report, TASAT 7.11 had not yet been evaluated by Schafer.

Preparations were made to enable color photometry data reduction and analysis to be performed in the Schafer offices. Background studies were performed in several areas to support the GLINT science team and the passive ID portion of GLINT – IR detectors, pattern recognition statistics and algorithms, and Fourier telescopy.

Implementation of pattern recognition algorithms for the passive identification of satellite bus structures with a probability of correct identification was completed. These algorithms utilize broadband Johnson B, V, R, I photometry. The algorithms that have been tested are k-nearest neighbor, Gaussian classifier, and Mahalanobis distance used with principal components analysis. The latest results are shown in Figures 4 through 6. Schafer also developed additional pattern recognition code to aide in the determination of an optimal data processing algorithm for the color photometry data. This information allowed the principal component classifier to be updated and refined.

Schafer traveled to Maui to attend the SILC (SOI In Living Color) BattleLab project kickoff meeting. This is a spectral photometry project with similar goals to the Signatures Program. Data analysis techniques developed for GLINT will be used in this project. This contract also supported the travel to Maui by Schafer to enable and support a color photometry experiment using the Advanced Electro-Optical System (AEOS) 3.6-m telescope.

Schafer efforts also included extending the photometric study into the Infrared under an initiative entitled Near IR Field Test (NIFTE). Infrared detectors, cameras, and spectrographs were researched and the information compiled was delivered to AFRL. General support was provided for the IR experiment plans. This included radiometric studies of the solar flux in the IR.

Schafer prepared a paper for the Space Control Conference in 1999 entitled "Color Photometry of GEO Satellites" which summarizes the Signature program's results for the contract period (Attch 2).

Activities related to advocacy of the color photometry technique at the Combined Intelligence Center (CIC) and the BattleLab initiative SOI In Living Color (SILC) have been reported under Task 109.

Relay Mirror Experiment

Schafer conducted a preliminary analysis of a proposed AFRL relay mirror experiment. After investigating several options, we recommended orbits to use for relay mirror experiments between Kirtland Air Force Base (AFB), NM and White Sands Missile Range NM, and between Kirtland AFB and Maui. Orbital propagation simulations were performed for experiments involving one or two relay mirrors between each pair of sites. These simulations showed how link availability, link ranges, and required beam turning angles and slew rates varied with relay mirror altitude. Schafer also wrote Matlab scripts to model laser propagation (using Fresnel diffraction calculations) through the relay mirror links. The models included the effects of wavefront error, jitter, and variable focusing by the transmitter and relay mirror optics. Schafer computed throughput efficiency and required laser pulse energy for a laser target designation demonstration. Finally, simulated images of tactical targets were created against a desert background to highlight target identification issues. This work was documented in a briefing presented

at the 23 June 1998 meeting of the AFRL relay mirror experiment working group (Attch 3).

Target Selection Database

Dr. Mara Payne (Schafer Corp.)
for
AFRL/DEBS GLINT Program

4 November 1998
GLINT TIM (Socorro)

Schafer

Target Selection Database

- Contains 697 GEOs
- Identifies GEOs visible from NM and Maui
- Includes estimate of visual magnitude for 10 solar phase angles
  - Radar cross-section converted to visual magnitude
  - Relation developed by John Lambert (Boeing) for GEOs
  - Limited to those GEOs with RCSs
- Work in progress

Schafer

Sample Data

SSC # 22911 Name: Solidaridad 1 Illumination ☐ Seen From: Maui ☑ Socorro ☑

BusStructure: HS-601 Status: Active

Inclination: 0.009 Stabilization: Three-axis - active Orbit: Geostationary

Revs/Day: 1.0027 Eccentricity: 0.0002 Degrees from Zenith: 39.4

Country: Mexico Description: COMM-CIVIL

Solar Phase Angle (degrees)	0	10	20	30	40	50	60	70	80	90
Estimated Magnitudes	10.9	11.3	11.7	12.1	12.4	12.7	13.0	13.3	13.5	13.8

SSC # 22930 Name: DBS 1 Illumination ☐ Seen From: Maui ☑ Socorro ☑

BusStructure: HS-601 Status: Active

Inclination: 0.003 Stabilization: Three-axis - active Orbit: Geostationary

Revs/Day: 1.0027 Eccentricity: 0.0002 Degrees from Zenith: 39.8

Country: USA Description: COMM-CIVIL

Solar Phase Angle (degrees)	0	10	20	30	40	50	60	70	80	90
Estimated Magnitudes	10.6	11.1	11.5	11.9	12.2	12.5	12.8	13.1	13.3	13.5

Schafer

Orbital Types

• **Type 1 GEOSTATIONARY** • Inclination less the 2 degrees • Eccentricity less than .1 • Revs per day between .9 and 1.1 • These objects stay roughly in the same part of the sky with little drift. Thus they are called GEO Stationary.	• **Type 3 GEO SYNCHRONOUS** • These objects have their revs per day between .9 and 1.1 so they have *some* synchronicity with the earth even though their eccentricity and inclination may cause it to be complicated. Thus they are called GEO Synchronous.
• **Type 2 GEO LONGISTATIONARY** • Inclination is greater to or equal to 2 degrees • Eccentricity is less than .1 • Revs per day between .9 and 1.1 • These are objects that, because of large inclination, have potentially a lot of north/south motion but stay over the same longitude. Thus they are called GEO Longistationary.	• **Type 4 DEEP SPACE** • These objects' revs per day are simply less than .9 so they are out beyond the GEO belt. Thus they are called Deep Space.

Schafer

Estimated Magnitudes

Deep Space Optical Catalog
Developed by John V. Lambert, Boeing North American - Space Operations Center, using optical and radar cross-section data collected at Maui on deep space objects. (1996)

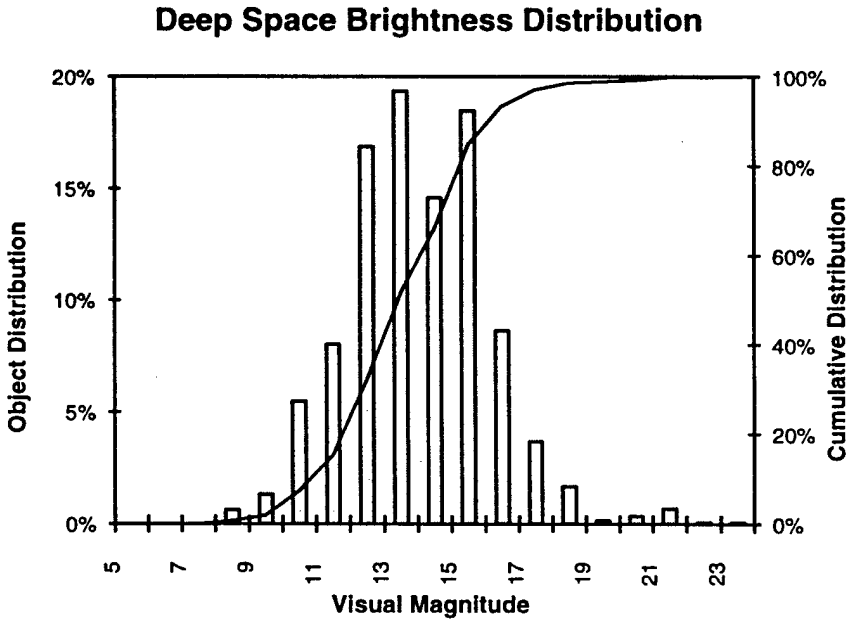

$M_v = M_{sun} - 2.5 \log [(a\ RCS)/(4\ \pi\ R^2)]$
where
M_{sun} = -26.74 visual magnitudes
a = Albedo = .20 (from earlier, unpublished analyses)
R = range

The estimated apparent magnitude was calculated for midnight September 22, 1997 using OPAS (Orbital Propagation Analysis Software).

Schafer

Color Photometry of GEO Satellites

T. E. Payne (Schafer), D. J. Sanchez (UPR), S. A. Gregory (UNM), L. G. Finkner (Boeing), E. Caudill (AFRL), D. M. Payne (Schafer), L. Kann (AFRL), C. K. Davis (Boeing)

Abstract

The Air Force Research Laboratory Directed Energy Directorate (AFRL/DE) Space Surveillance Technologies Branch is pursuing non-imaging techniques to obtain information on the identity and status of geosynchronous (GEO) satellites. On-going experiments have provided visible color photometry data on several GEO satellites for space object identification (SOI) purposes. These data have been analyzed using statistical probabilities to produce quantified identifications of satellite bus types and the satellites themselves. Additional analysis has been performed to ascertain the relative usefulness of each photometric bandpass in order to optimize this color photometry technique. The results and conclusions of this work to-date are presented

Introduction

GEO satellites pose unique challenges to the Space Surveillance Network to track, identify, and to determine anomalous behavior because the majority of them are three-axis stabilized and have no relative motion with respect to the observer. This stability makes radar tracking and imaging not feasible unless the satellite has become unstable, parts of the satellite move, or the orbit is not truly geosynchronous. Therefore, optical tracking and photometric signatures are the tools that are used most often to track, identify, and determine status or anomalies. Space object identification (SOI) of GEO satellites is a difficult task given the faint, unresolved character of the optical signal. Surveillance deficiencies have been identified related to detection of changes of status of GEO, anomaly resolution, general GEO intelligence, and the lack of global coverage. SOI needs include identification of class and type, status determination (operational or not), and anomaly resolution. Potential solutions have been identified with color photometry as one possibility to aide in resolving cross-tags and status determination. [1]

Color photometry, also known as multi-spectral photometry, and in some circles as hyperspectral which connotes very narrow bands has its origins in astronomy. Astronomical photometry is defined as the measurement of the apparent brightnesses of an object in various wavelength bands in the optical or infrared regions of the electromagnetic spectrum. The brightnesses are usually referred to in magnitudes where $m_1 - m_2 = -k \log_{10}\left(\frac{f_1}{f_2}\right)$. The magnitudes assigned to the objects are m_1 and m_2 with energy fluxes f_1 and f_2 and k is a constant. The minus sign is chosen so that brighter objects have smaller numeric values of m. Since the definition of magnitude involves two objects, magnitude is a relative concept. If a photometric system with several filter bands at different wavelengths is used, by taking the difference in magnitudes measured in two different bands, color or a color index can be formed. For instance, if the standard Johnson broadband filter system is used, the filter bands are denoted U, B and V. The wavelengths corresponding to those bands are shown in Figure 1. Then a color index can be defined as

$$B - V = K - 2.5 \log \frac{\int_0^\infty F_B(\lambda) d\lambda}{\int_0^\infty F_V(\lambda) d\lambda}$$

; where K is a constant. F_x is the observed energy flux through filter x. In reality, the infinite integral is cutoff by the finite extent of the filter bandpass. So a color index essentially measures the ratio of flux between characteristic wavelengths. [2] A larger numerical value for the color index indicates a redder color, while a smaller numerical value indicates bluer color.

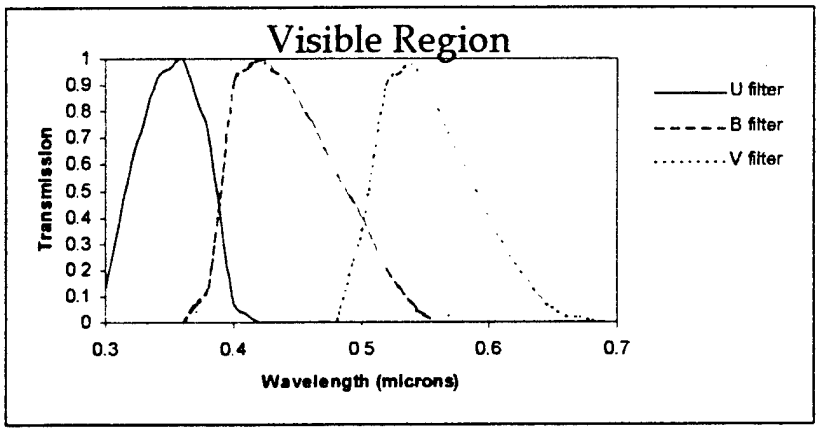

Figure 1. Standard Johnson filter bands U, B, V

Previous work supported by the AFRL Directed Energy Directorate (DE) on simulations of spectral signatures (reflected electromagnetic spectrum off GEO satellites) concluded that color photometry was a promising technique for addressing problems in GEO SOI. [3] [4] Additionally, color photometry observations were sponsored by AFRL/DE showing that different satellites had different color characteristics. [5] Prior photometric works by John V. Lambert (Boeing) and W. I. Beavers (MIT/LL) have also shown that information about the satellite was available in the brightnesses and the colors. The difficulty in any optical non-imaging technique is how to exploit that information and yield quantified variables about the satellite's identity and status. This has been the goal of the current on-going effort supported by AFRL/DE.

The current work presented here has endeavored to classify the satellite type by using its photometric colors. The extended standard Johnson system has been used to-date. These filters are designated B, V, R, and I. The properties of these filters are summarized in Table 1. [6] The current observations are being made at the Capilla Peak Observatory (CPO) outside of Albuquerque, NM. The U filter has not been used to-date due to lack of transmission at these wavelengths at this observatory. The current set of observations span from June 1998 to the present. As of this writing, 175 observations have been taken on 10 satellites, some of which are in a cluster. Table 2 contains the list of satellites.

Table 1. Johnson Filter Characteristics

Filter	Mean Wavelength (μ)	FWHM (μ)
B	4417	960
V	5505	827
R	6690	1744
I	8000	1425

Table 2. Satellites.

Satellite Name	Type
Solidaridad 1	Hughes 601
Solidaridad 2	Hughes 601
Anik E1	GE Satcom 5K
Anik E2	GE Satcom 5K
DBS 1	Hughes 601
DBS 2	Hughes 601
DBS 3	Hughes 601
AMSC 1	Hughes 601
Gstar 4	LMAS 3000
Spacenet 4	LMAS 3000

Data Reduction and Analysis

The data is obtained using a CCD camera with the B, V, R, and I filters. Observations of stars are made for radiometry and color calibrations. Sky flat fields, bias, and dark frames are taken and used in the data reduction to minimize noise and errors in the photometric data. The instrumental magnitude is calculated using the Image Reduction and Analysis Facility (IRAF) software package. IRAF contains a large selection of computer programs for general image processing, reduction and analysis of optical and IR CCD data. [7] The instrumental magnitude ($m_{instrument}$) in obtained by measuring the intensity on (I_{on}) and off (I_{off}) the object of interest using the IRAF software and using the relation

$$m_{instrument} = -2.5\log\left(\frac{(I_{on} - I_{off}) \times N_{pixels}}{t_{exposure}}\right)$$; where N_{pixels} is the number of pixels subtended by the object and $t_{exposure}$ is the exposure time of the observation. The instrumental magnitude is then converted to a standard magnitude using a relation between the standard magnitude and the instrumental magnitude as shown in Figure 2. All other filters are similarly treated. This process removes the effects of the Earth's atmosphere and the telescope. The final standard magnitudes have an uncertainty of .03 magnitudes and are exoatmospheric

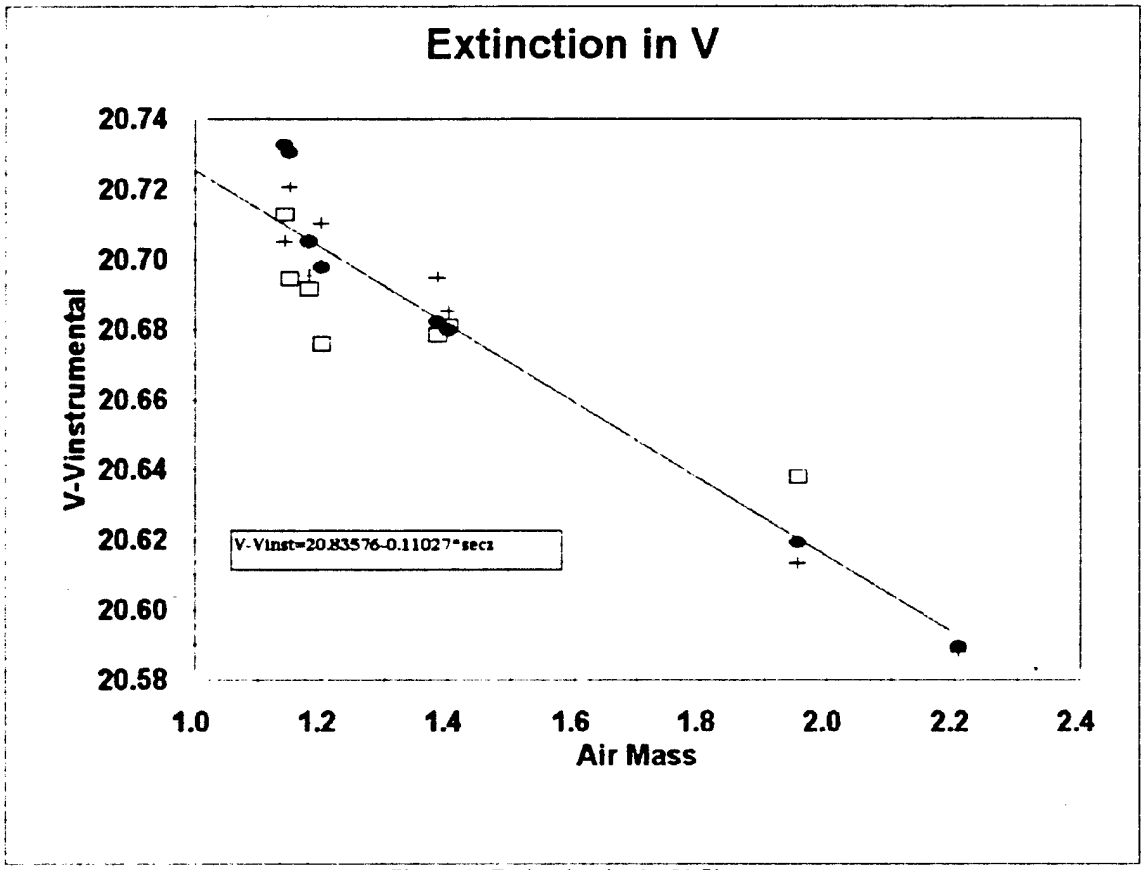

Figure 2. Extinction in the V filter.

Photometric Analyses and Results

As can be seen in Table 2, all the satellites under consideration are three-axis stabilized. Their features are very similar as is apparent in Figure 3. The color photometry data taken on these satellites was processed using two different types of groupings. One group separates the 10 satellites into 3 classes by type of

payload. The second group separates the satellites into 5 classes by type of satellite. Table 3 shows these groupings.

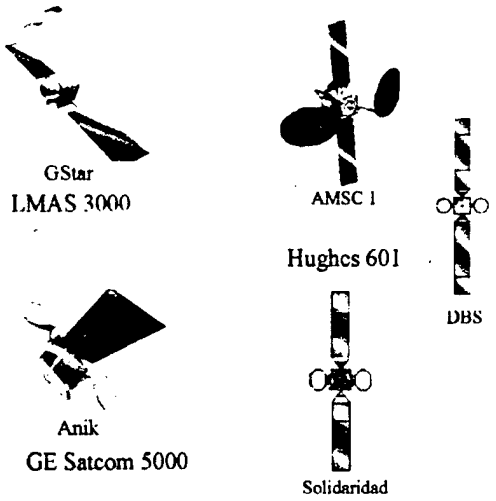

Figure 3. Depictions of some of the satellites.

Table 3. Satellite groupings.

Satellite Name	Type	Group 1	Group 2
Solidaridad 1	Hughes 601	1	1
Solidaridad 2	Hughes 601	1	1
DBS 1	Hughes 601	1	4
DBS 2	Hughes 601	1	4
DBS 3	Hughes 601	1	4
AMSC 1	Hughes 601	1	5
Anik E1	GE Satcom 5K	2	2
Anik E2	GE Satcom 5K	2	2
Gstar 4	LMAS 3000	3	3
Spacenet 4	LMAS 3000	3	3

For illustrative purposes, Figures 4 - 5 plot the data when magnitudes and colors are plotted against one another The data is plotted using Group 1 designations. By themselves, these data do not separate out the satellite classes completely

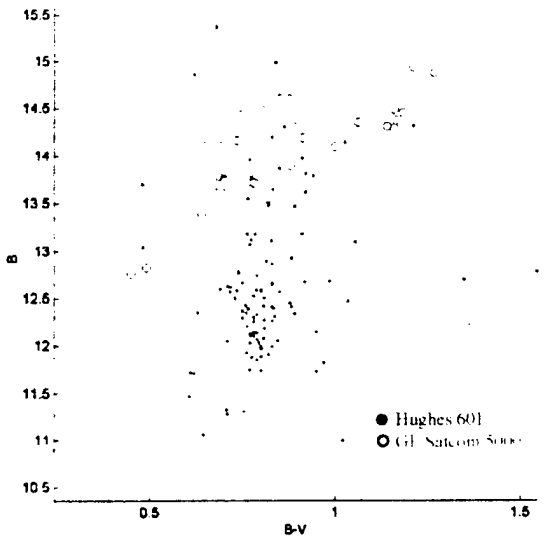

Figure 4. Color-Magnitude Plot

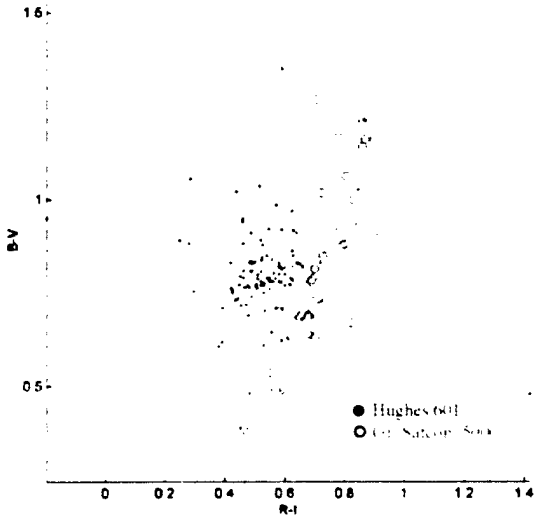

Figure 5 Color-Color Plot

Therefore, it was determined that pattern recognition algorithms may be applicable to this problem and may separate the classes better. In addition, the application of these algorithms would enable quantified confidence levels to be calculated on the ability to correctly identify the satellite class. Three different discriminants or classifiers are currently being tested: K-nearest neighbor, Gaussian classifier, and Mahalanobis distance. These are each used in combination with principal component analysis to obtain a percentage of correct identification of each group. A brief description of each algorithm follows.

In pattern recognition terminology, the magnitude and color data creates a feature space. A feature space is defined by the different features of the data. These features describe the data in terms that are of interest for a specific problem. For instance, medical data on people can define a feature space whose dimensions are height, weight, age, and sex. In this case, the dimensions of our feature space are the magnitudes B, V, R, I, and the colors, B-V, V-R, and R-I. Feature space, in general, is a n-dimensional space that is defined by the properties that describe the population of interest.

Principal component analysis is a common type of preprocessing that aims at reducing the number of input variables or the dimensions of the feature space while maintaining the most significant relationships reflected by the data. This technique attempts to identify an m-dimensional subspace of the n-dimensional feature space that seems most significant, and then projects the data onto this subspace. [8]

K-nearest neighbor is a classifier in which the position in feature space of the k-nearest neighbors whose identities are known is compared with the position of the data point whose identity is to be determined. This relative position is used to determine the identity of the unknown data point, where k is an integer variable ranging from 1 to the number of data points minus one. With the current data, the best results are obtained when $k = 3$. For example, if the three closest data points in the feature space to the unknown data point are identified as Hughes 601 (using Group 1), then the unknown data point is identified as Hughes 601 with 100% probability.

The Gaussian classifier fits a Gaussian with a mean and standard deviation in feature space to each class. An unknown data point's location in feature space is then compared with the position, shape, and extent of the Gaussians in the feature space. If the unknown data point is at a location in feature space that is described by only one Gaussian, then its identity is known to 100% probability. If that location is shared by two Gaussians, then the Euclidean distance from the mean of each Gaussian is computed and relative probabilities are generated that the unknown data point belongs to each population represented by each Gaussian. [9]

The Mahalanobis distance is used in the algorithm above instead of the Euclidean distance. When the Gaussian classifier is used, there is a possibility of error unless all the Gaussians have the same shape and extent and the probabilities are equal that the unknown data point is any of the classes. So, classification based on the nearest Gaussian may be near optimum only if appropriate additional weights are introduced by using a Mahalanobis distance. [10]

These color photometry data were processed using the above techniques. Their results were then studied to determine which filter combinations, groups, and classifiers yielded the best results. When the data was combined using Group 2, the results were much poorer than when the data was combined using Group 1. One major factor is the limited amount of observations. The results for Group 1 using the three classifiers are shown in Figures 6 - 8. They show correct identification using k-nearest neighbor, 81.14% using the Gaussian and 86.29% using the Mahalanobis distance. The results for Group 2 using k-nearest neighbor are 52.00% correct identification, using a Gaussian they are 45.71%, and the results are 55.43% using the Mahalanobis distance.

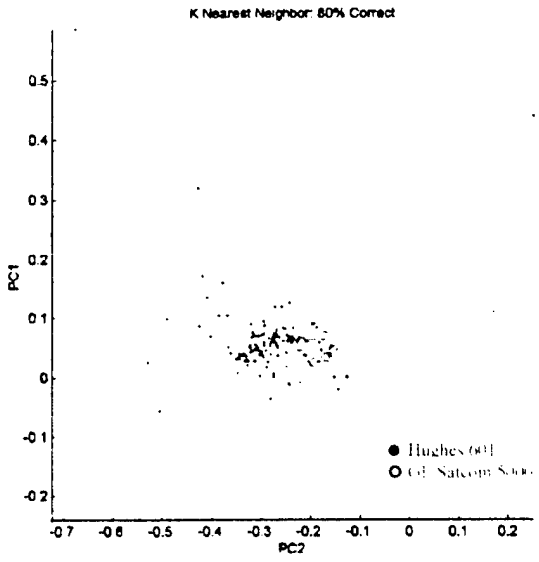

Figure 6. K-nearest neighbor (k=3).

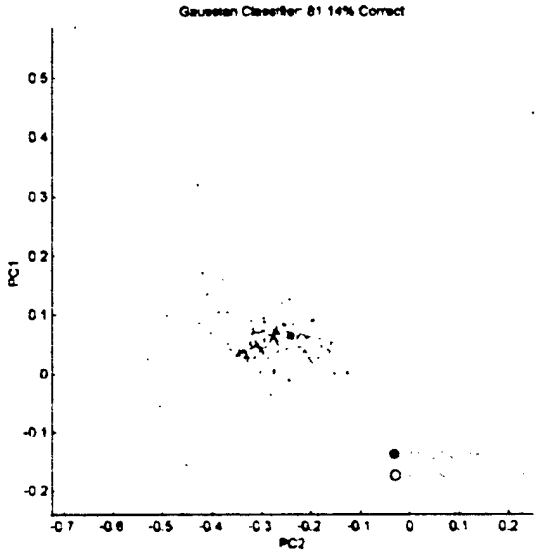

Figure 7 Gaussian classifier

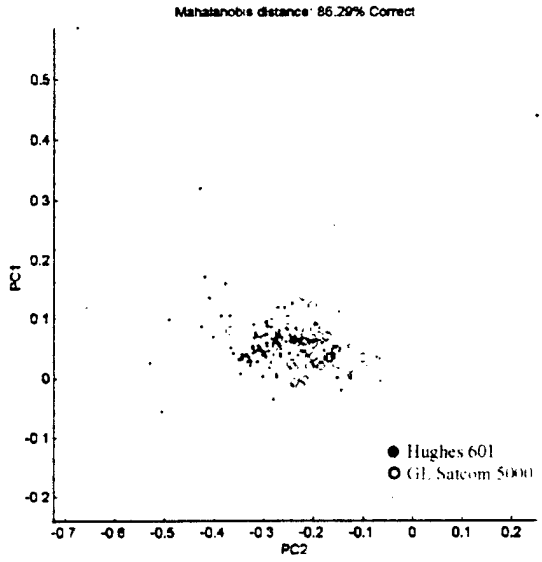

Figure 8. Mahalanobis distance.

Conclusions

Our results show that there is utility in color photometry data of GEO satellites and that the information can be obtained to achieve identification with a good probability. This technique shows promise in minimizing and correcting cross-tags. Because of the limited amount of data, plans have been made to continue to take color photometry of these satellites in the filters discussed here. No one filter combination stood out as yielding more information than the others. Plans have been made to obtain color photometry data using different filters in addition to the current ones. These new filter characteristics were designed from the information obtained from the spectral simulations previously cited and from the work of Poelman. [3] [4] [11] The detailed shape of an energy distribution (i.e. spectrum) is determined by a few basic physical parameters. By an astute choice of filters, features in the energy distribution that are sensitive to these parameters can be isolated. [2] Further efforts are in the areas of pattern recognition algorithm development, incorporation of solar and sensor angles (phase angles) into the feature space, the continued development of a color photometric database, and the possibility of photometry in other regions of the spectrum. Some of this work will be in collaboration with the Space Battlelab initiative SOI In Living Color (SILC). The goal of these efforts is threefold: first, to obtain the ability to identify active payloads; second, to be able to provide a tip-off of anomalous behavior; and finally, to be able to provide information on dead satellites, i.e. to provide some information on what is wrong.

References

1. Benedict, R., Optical Network Mission Study 1996 - 1997 Final Report, Jointly sponsored by Air Force Space Command and Air Force Research Laboratory.
2. Mihalas, D. and Binney, J., Galactic Astronomy, 2nd ed., W. H. Freeman and Co., San Francisco, 1981.
3. Payne, T. E., *et al.*, Modeling of Spectral Signatures from Geosynchronous Satellites (U), *MIT/LL Space Surveillance Workshop*, 1996, SECRET.
4. Payne, T. E., *et al.*, Analysis of Simulated Spectral Signatures from Geosynchronous Satellites (U), *MIT LL Space Control Conference*, 1997, SECRET.
5. Gregory, S. A., CCD Observations of Geosynchronous Satellites, Final Report, August 1997.
6. Beckert, D. C., and Newberry M. V., The Design and Testing of Filter-Detector Systems Using Synthetic Photometry, *P.A.S.P.*, 101, 849-858, Sept., 1989.
7. http://iraf.noao.edu/
8. Kennedy, R. L., *et al.*, Solving Data Mining Problems Through Pattern Recognition, Prentice Hall, Upper Saddle River, NJ, 1997.

9. Rogers, S. K., and Kabrisky, M., An Introduction to Biological and Artificial Neural Networks for Pattern Recognition, SPIE, Bellingham, WA, 1991.
10. Pao, Yoh-Han, Adaptive Pattern Recognition and Neural Networks, Addison-Wesley, Reading, MA, 1989.
11. Poelman, C. J., and Meltzer, S. R., Spacecraft Identification By Multispectral Signature Analysis Using Neural Networks, PL-TR-97-1053, March 1997.

Schafer

Bifocal Relay Experiment

Dustin Johnston
Tom Brown
Bob O'Leary
Don Payne

23 June 98

Schafer

Outline

- SOR to WSMR Relay Mirror Experiment
  - 1-Bounce Relay
    - » Beam turning angle issue
    - » Link availability
    - » Throughput
  - 2-Bounce Relay
    - » Link availability
- SOR to Maui Relay Mirror Experiment
  - 1-Bounce Relay
    - » Link availability
    - » Throughput
  - 2-Bounce Relay
    - » Link availability
- Imaging / target identification issues

Schafer

SOR to WSMR Relay

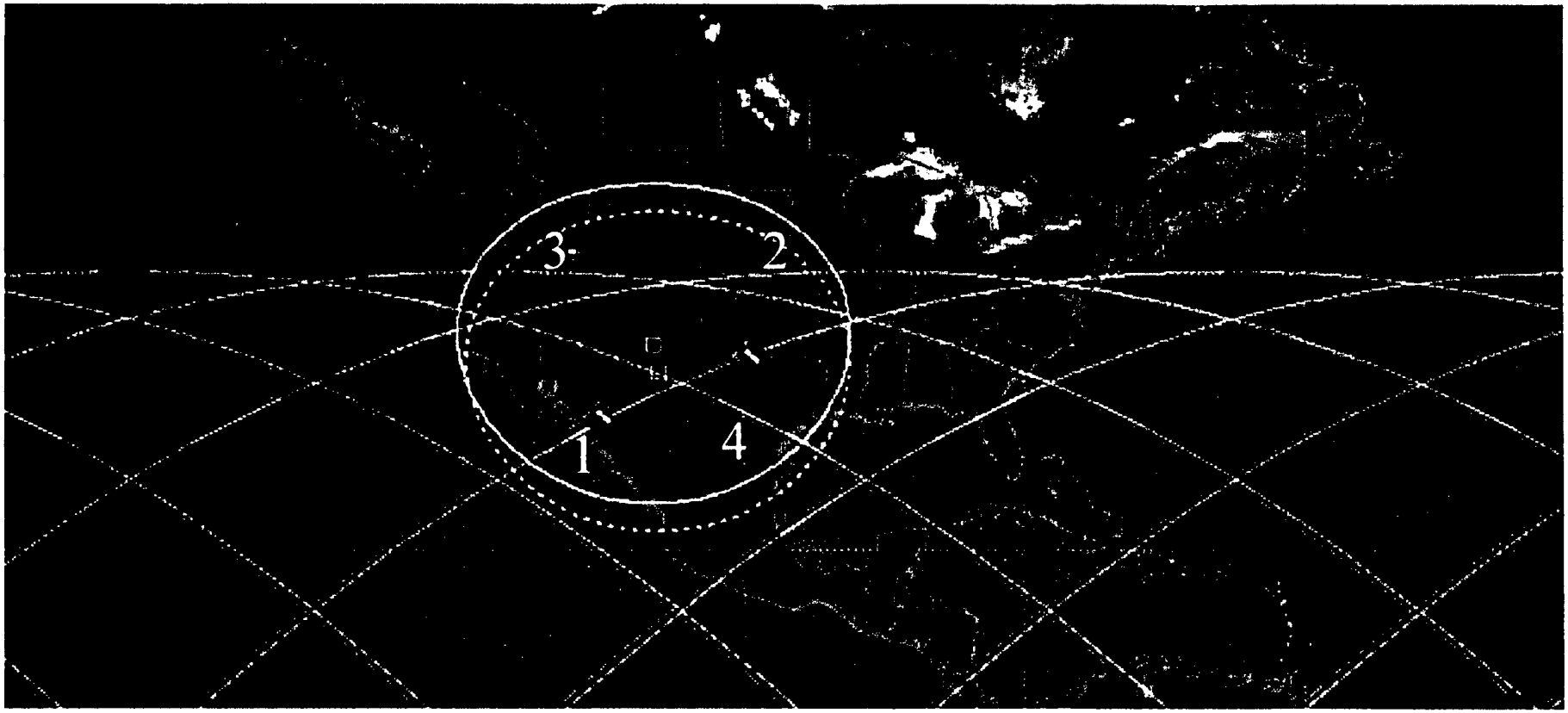

Minimum elevation angle at both sites: 30°
Altitude = 1000 km

SOR to WSMR 1-Bounce Relay

- Sharp beam-turning angle

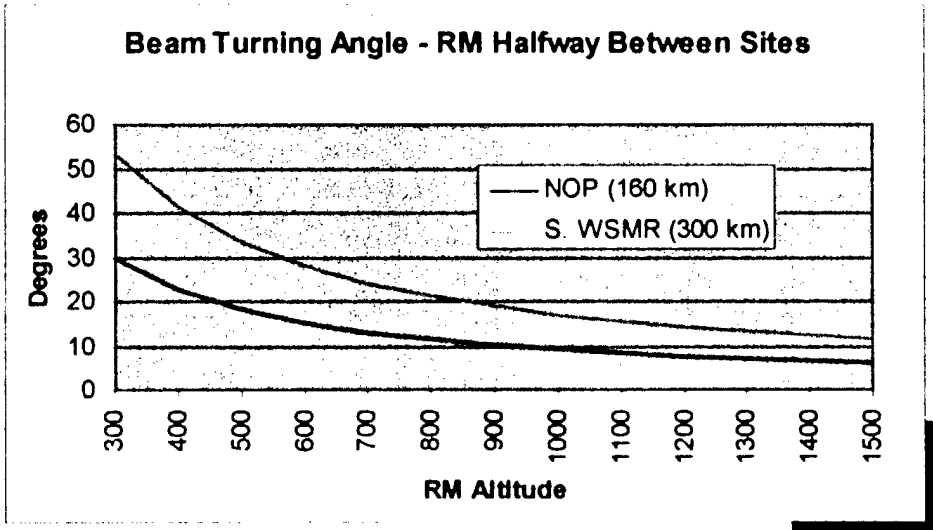

- Altitude: 500 km
- Inclination: 40°

- Results of 1-year simulation (1-minute time steps)
  - Average link open 3.9 minutes
  - Average uplink: 677 km
  - Average downlink: 709 km
  - Average beam turning angle: 25°
    - » Minimum: 15 °
  - Maximum slew rate: 188 μrad/s

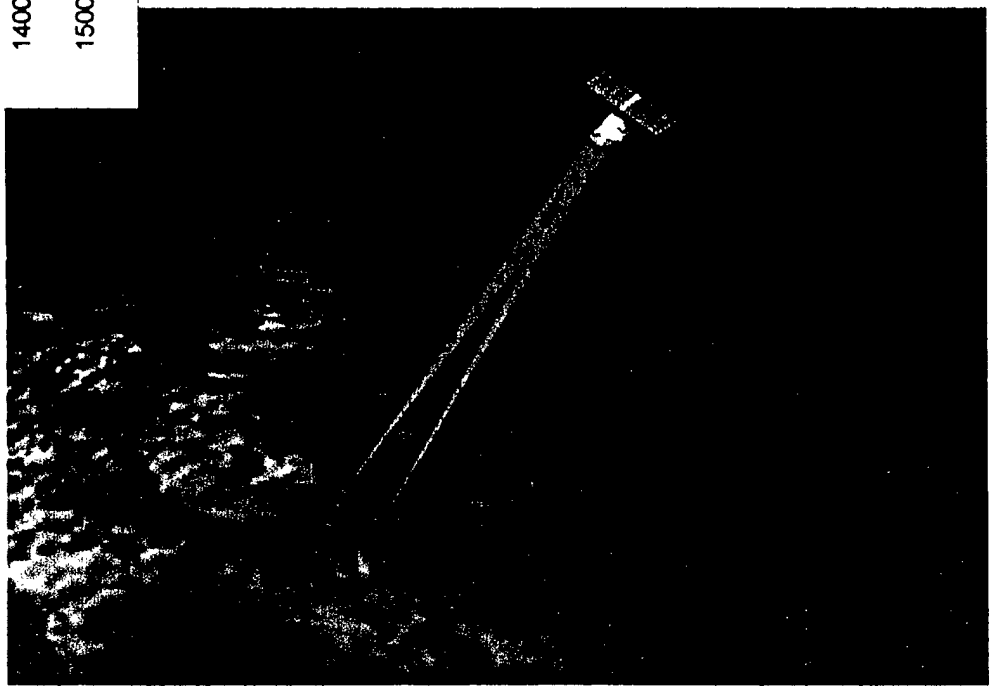

Schafer

SOR to WSMR 1-Bounce Relay
Satellite Altitude vs. Link Availability

- Inclination: 40°
- Minimum elevation angle: 30°

	Satellite Altitude		
	500 km	1000 km	1500 km
Links / year	1108	1641	1668
Average link time	3.9 min	7.6 min	11.1 min

Schafer

Minimizing Diffraction Loss

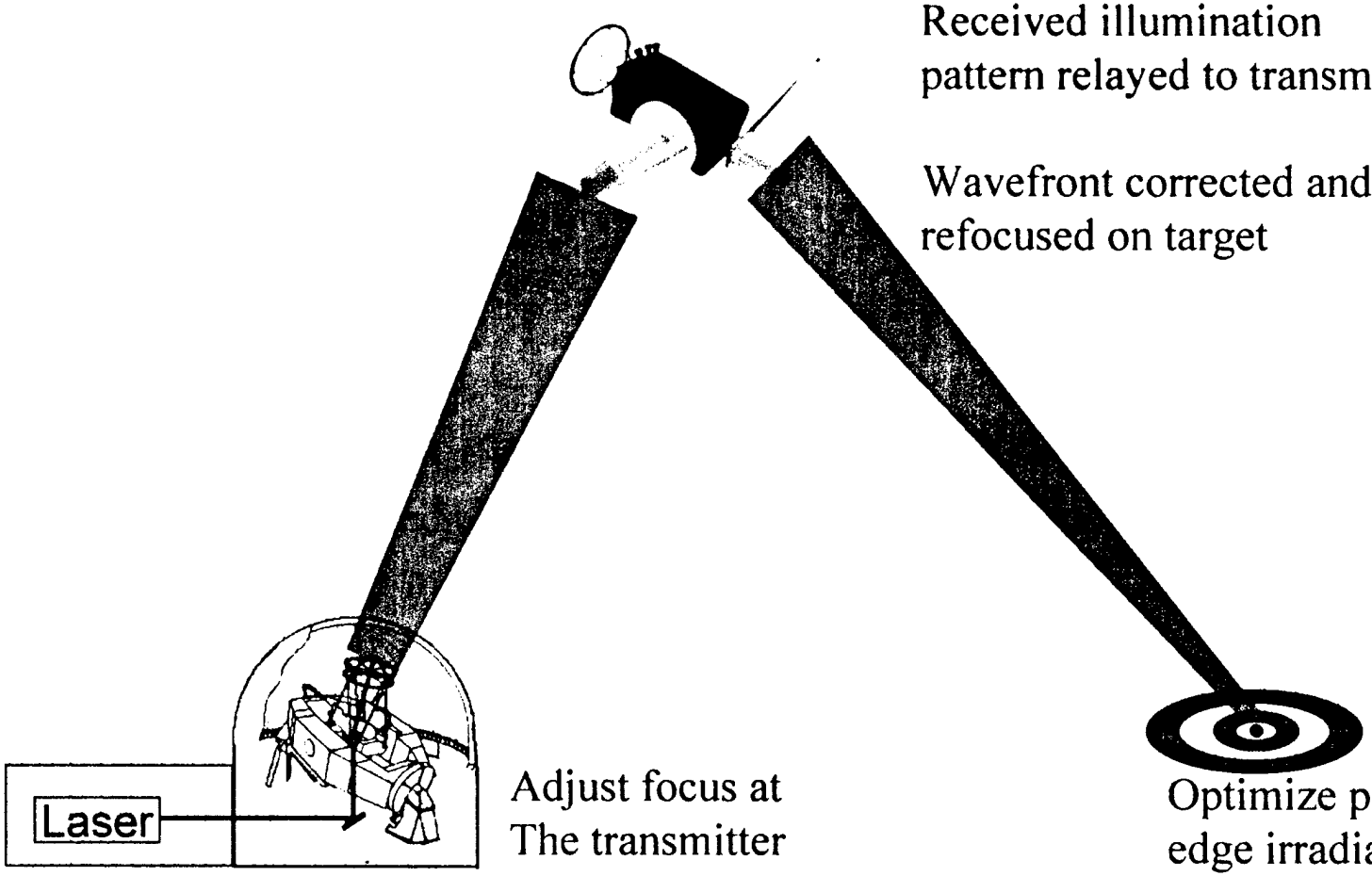

Source: John Erkkila, Logicon RDA

Schafer

Target Irradiance / Fluence at Edge of 1-m Spot

SOR 1-bounce relay to WSMR

Transmitter diameter = 3.5 m
λ = 1 μm
Uniform illumination of xmtr aperture
No jitter or wavefront error

Transmitter optics transmission = 0.6
Bifocal optical transmission = 0.8
Atmospheric transmission each way: 0.8

Xmtr focus adjusted to maximize edge fluence at tgt (Fresnel diffraction calculation)
Relay mirror focused at target

Uplink range = downlink range

		500 km	1000 km	1500 km
Relay mirror diameter	1 m	$1.1\ 10^{-5}$	$8.6\ 10^{-6}$	$4.6\ 10^{-6}$
	1.5 m	$6.5\ 10^{-6}$	$1.1\ 10^{-5}$	$8.3\ 10^{-6}$

W/cm^2 per watt transmitted
J/cm^2 per J/pulse transmitted

Schafer

Link Efficiency
SOR 1-bounce relay to WSMR

Transmitter diameter = 3.5 m
λ = 1 μm
Uniform illumination of xmtr aperture
No jitter or wavefront error

Transmitter optics transmission = 0.6
Bifocal optical transmission = 0.8
Atmospheric transmission each way: 0.8

Xmtr focus adjusted to maximize edge fluence at tgt (Fresnel diffraction calculation)
Relay mirror focused at target

Uplink range = downlink range

		500 km	1000 km	1500 km
Relay mirror diameter	1 m	0.24	0.089	0.040
	1.5 m	0.38	0.22	0.085

Fraction of transmitted pulse energy inside 1-meter spot at target

Schafer

Target Designation Application

- At LASSOS Kickoff Meeting, a typical laser target designator pulse energy was given as 100 mJ / pulse
- Conservatively, assume we need this much energy per pulse in the laser spot for the relay mirror experiment
  - Future work should include modeling target reflectivity, sensor, and engagement geometry
- The table below gives required transmitter pulse energies based on link efficiencies given in previous chart

		Uplink range = downlink range		
		500 km	1000 km	1500 km
Relay mirror diameter	1 m	410 mJ	1.1 J	2.5 J
	1.5 m	270 mJ	450 mJ	1.2 J

Schafer

SOR to WSMR 2-Bounce Relay

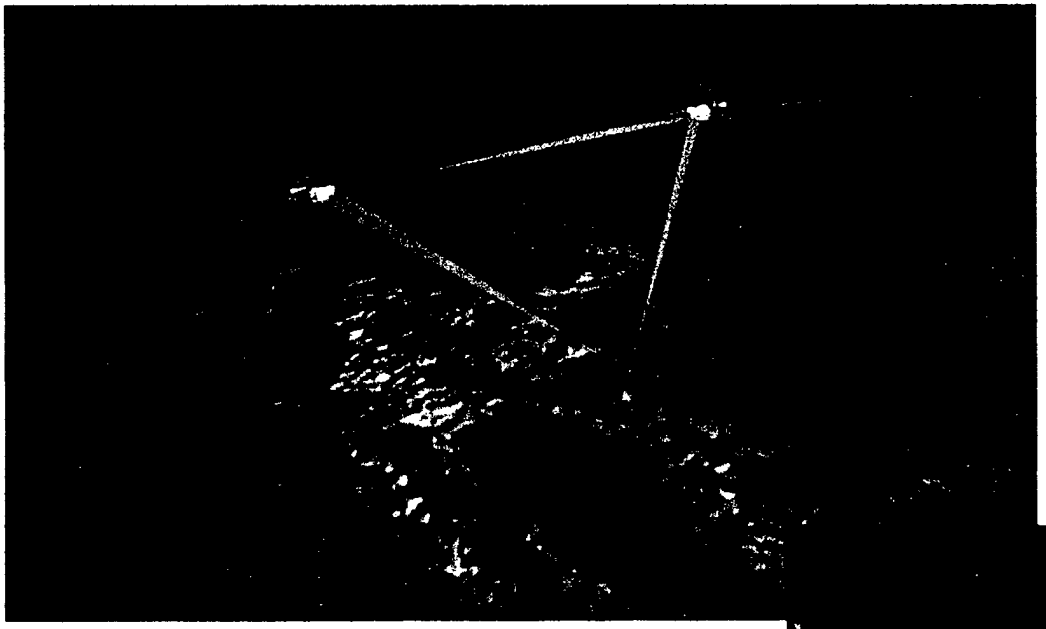

- Altitude: 500 km
- Inclination: 40°
- Satellite separation: 6°
  - ~ 720 km

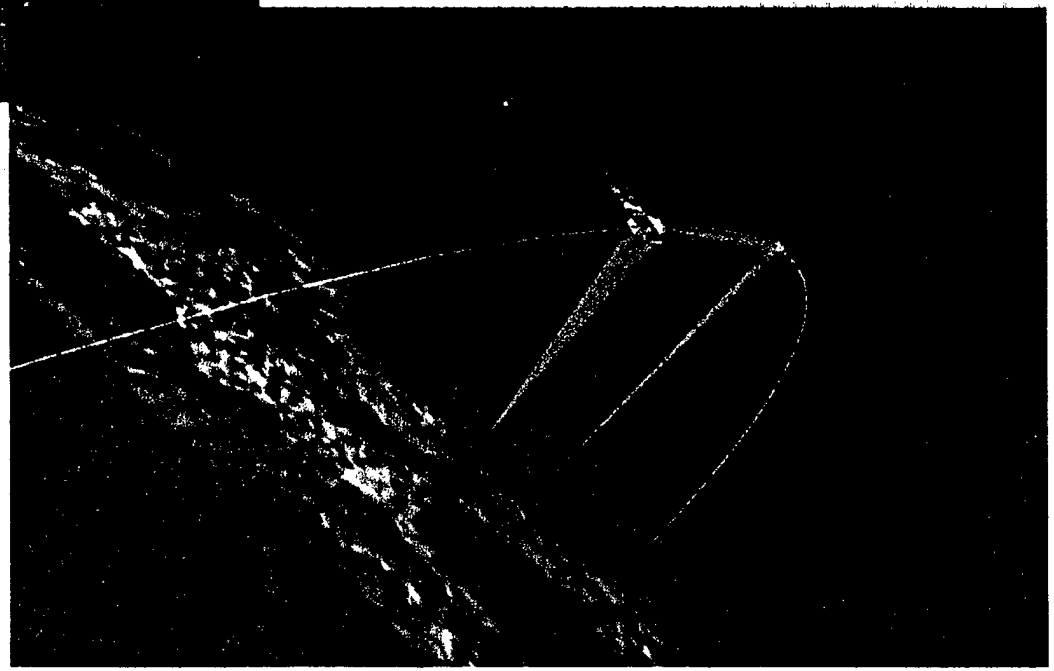

- Results of 1-year simulation (1-minute time steps)
  - Average link open 1.9 minutes
  - Average uplink: 712 km
  - Average downlink: 722 km
  - Average beam turning angle: 61°
  - Maximum slew rate: 715 μrad/sec

Schafer

SOR to WSMR 2-Bounce Relay
Satellite Altitude vs. Link Availability

- Inclination: 40°
- Satellite separation: 6° (~ 720 km)
- Minimum elevation angle: 30°

	Satellite Altitude		
	500 km	1000 km	1500 km
Links / year	987	1624	1664
Average link time	1.9 min	4.9 min	8.0 min

Schafer

Link Efficiency
SOR 2-bounce relay to WSMR

Transmitter diameter = 3.5 m
λ = 1 μm
Uniform illumination of xmtr aperture
No jitter or wavefront error

Transmitter optics transmission = 0.6
Bifocal optical transmission = 0.8
Atmospheric transmission each way: 0.8

Transmitter focused at first relay mirror, which is focused at second relay mirror
Second relay mirror focused at target

- Results for 1000-km up and downlink; 750-km crosslink
  - Fraction of transmitted pulse energy inside 1-meter spot at target
    - » 1.0-meter relay mirror: 0.043
    - » 1.5-meter relay mirror: 0.12
  - Energy per pulse required at transmitter to put 100 mJ on target
    - » 1.0-meter relay mirror: 2.3 J
    - » 1.5-meter relay mirror: 830 mJ

Schafer

Access Time Per Pass for One & Two Satellite Relay From SOR to WSMR

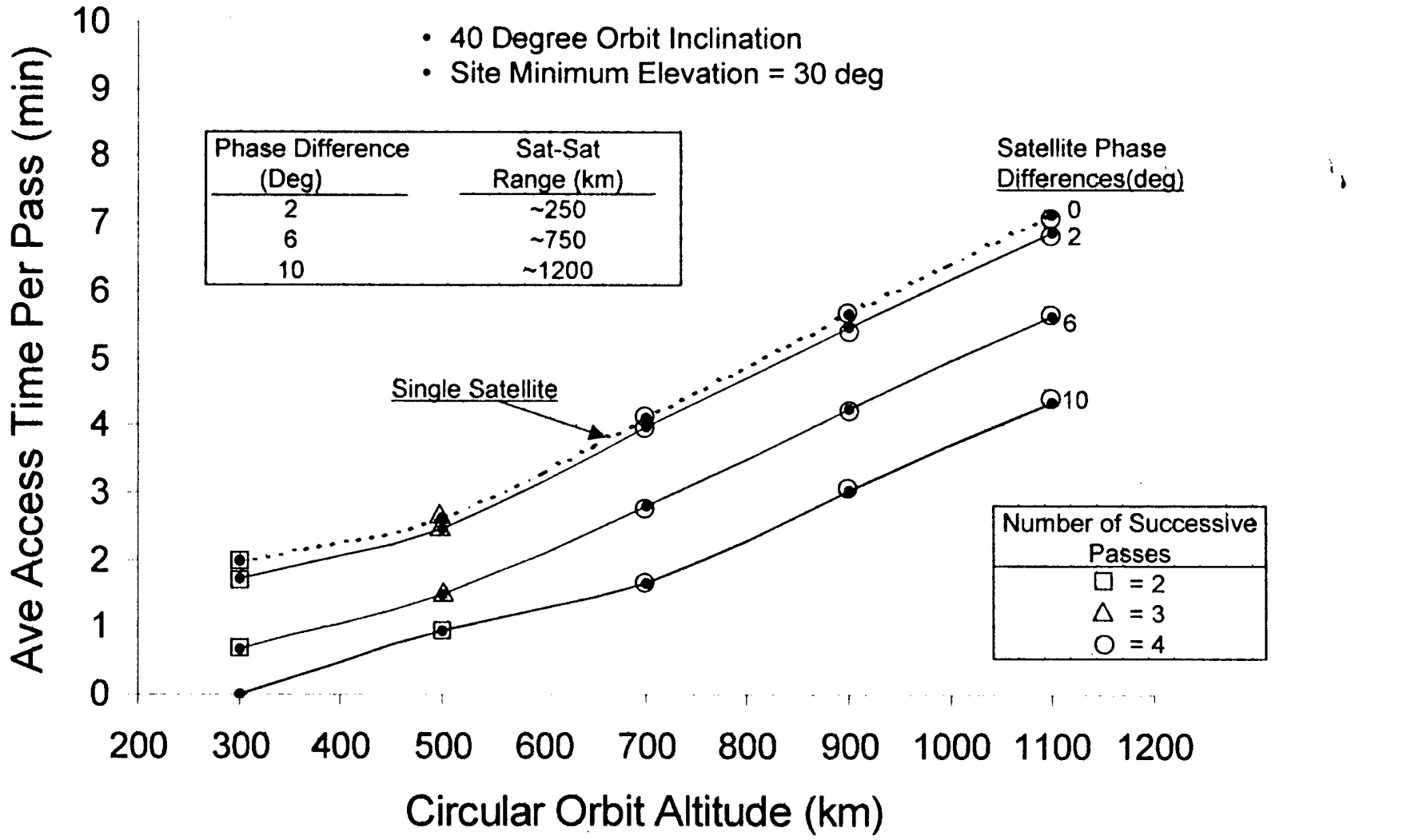

Data from 24-hour STK run

Schafer

Access Time Per Pass For Single Satellite Relay From SOR to MAUI

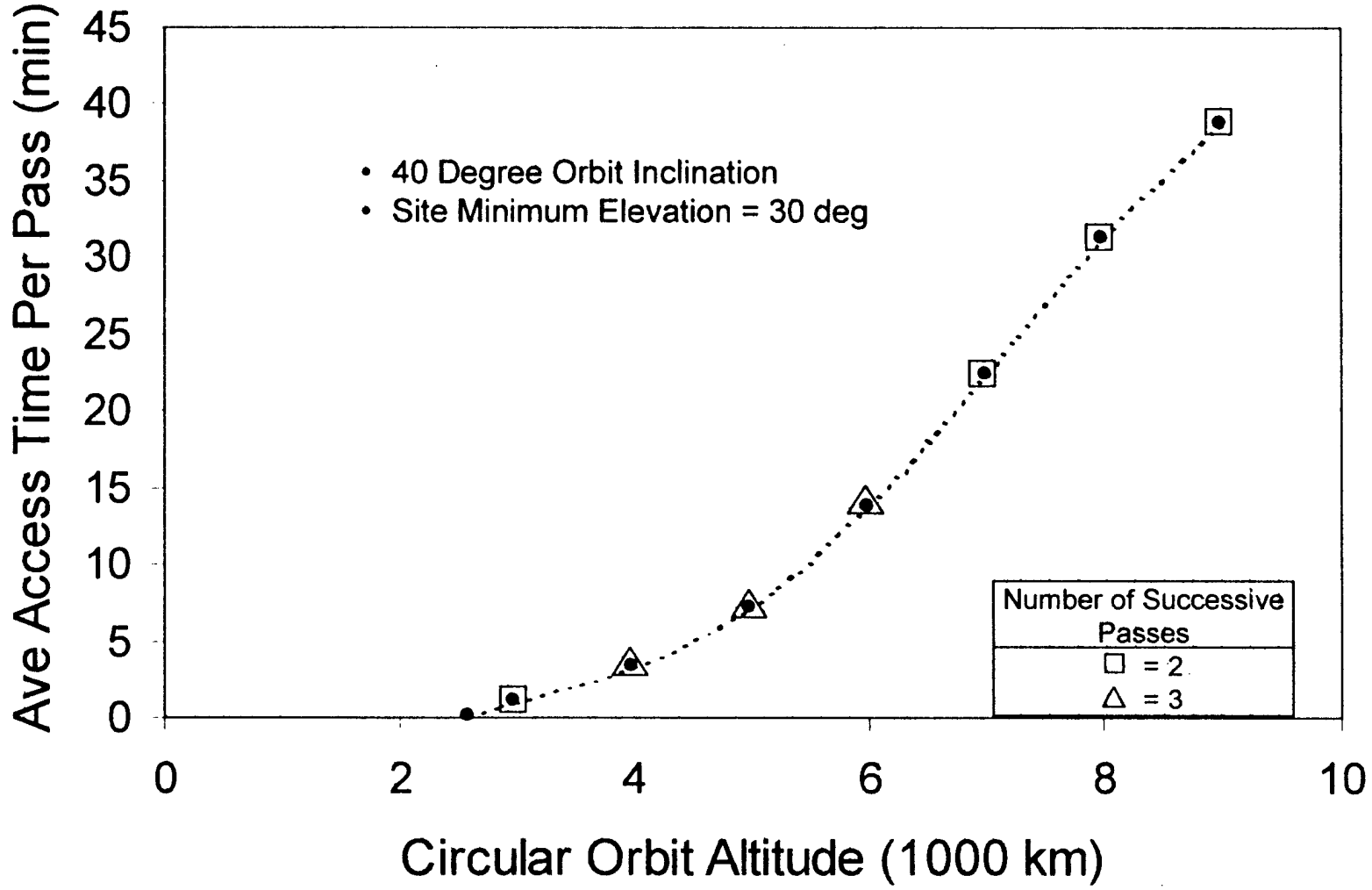

Note: Radiation shielding is a design issue

Data from 24-hour STK run

Schafer

SOR to Maui 1-Bounce Relay
Link Availability

- Orbit / link parameters
  - Inclination: 40°
  - Altitude: 5000 km
  - Minimum elevation angle: 30°
- Results of 1-year simulation (1-minute time steps)
  - Link availability (not including PCFLOS)
    - » Number of valid links per year: 1964
    - » Average link is open 9.6 minutes
  - Relay mirror design drivers
    - » Maximum uplink/downlink: 6758 km
    - » Maximum total range: 13489 km
    - » Minimum beam turning angle: 43.5 °
      - Average: 47.4 °
    - » Maximum slew rate: 31.6 μrad / sec

Schafer

Target Irradiance / Fluence at Edge of 1-m Spot

SOR 1-bounce relay to Maui

Transmitter diameter = 3.5 m
λ = 1 μm
Uniform illumination of xmtr aperture
No jitter or wavefront error

Transmitter optics transmission = 0.6
Bifocal optical transmission = 0.8
Atmospheric transmission each way: 0.8

Xmtr focus adjusted to maximize peak fluence at tgt (Fresnel diffraction calculation)
Relay mirror focused at target

Uplink range = downlink range

		5000 km	6000 km	7000 km
Relay mirror diameter	1 m	$2.2\ 10^{-7}$	$1.1\ 10^{-7}$	$6.8\ 10^{-8}$
	1.5 m	$8.6\ 10^{-7}$	$5.4\ 10^{-7}$	$3.0\ 10^{-7}$

W/cm^2 per watt transmitted
J/cm^2 per J/pulse transmitted

Based on calculations by John Erkkila, Logicon RDA

Schafer

Link Efficiency
SOR 1-bounce relay to Maui

Transmitter diameter = 3.5 m
λ = 1 μm
Uniform illumination of xmtr aperture
No jitter or wavefront error

Transmitter optics transmission = 0.6
Bifocal optical transmission = 0.8
Atmospheric transmission each way: 0.8

Xmtr focus adjusted to maximize peak fluence at tgt (Fresnel diffraction calculation)
Relay mirror focused at target

Uplink range = downlink range

		5000 km	6000 km	7000 km
Relay mirror diameter	1 m	0.0017 (58 J)	0.00086 (120 J)	0.00054 (190 J)
	1.5 m	0.0070 (14 J)	0.0043 (23 J)	0.0024 (42 J)

Fraction of transmitted pulse energy inside 1-meter spot at target
(Energy per pulse required at transmitter to put 100 mJ on target)

Radiation Environment Considerations

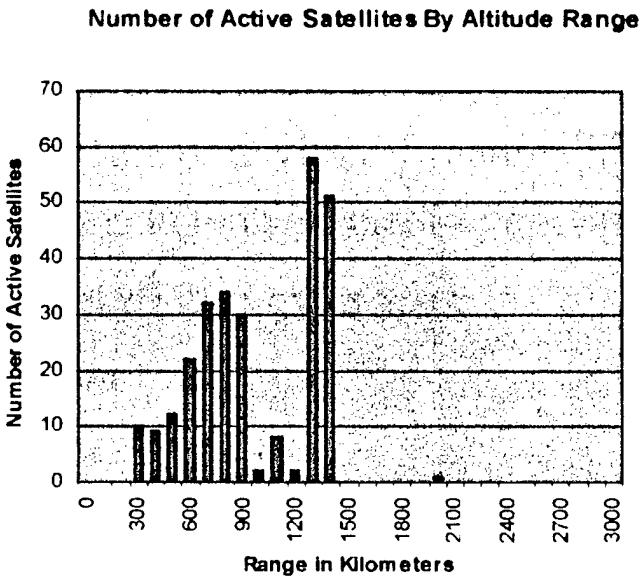

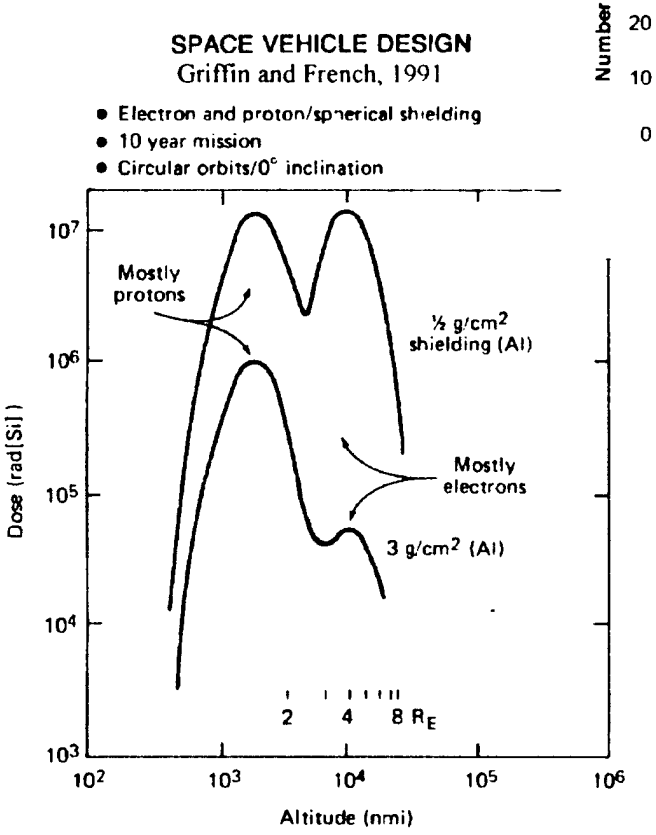

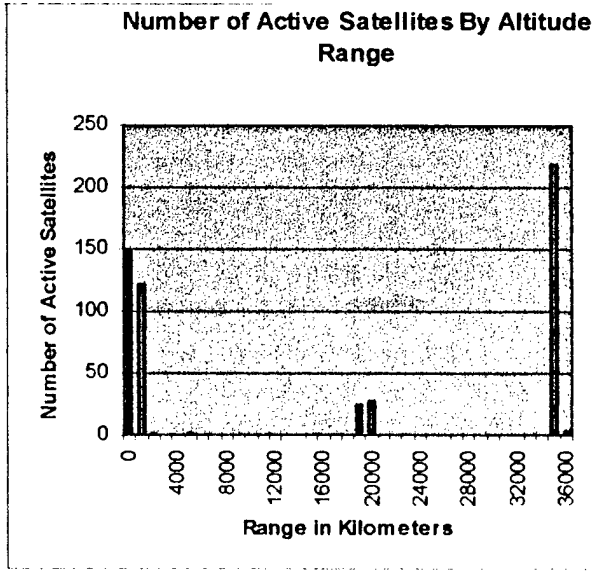

Schafer

SOR to Maui 2-Bounce Relay

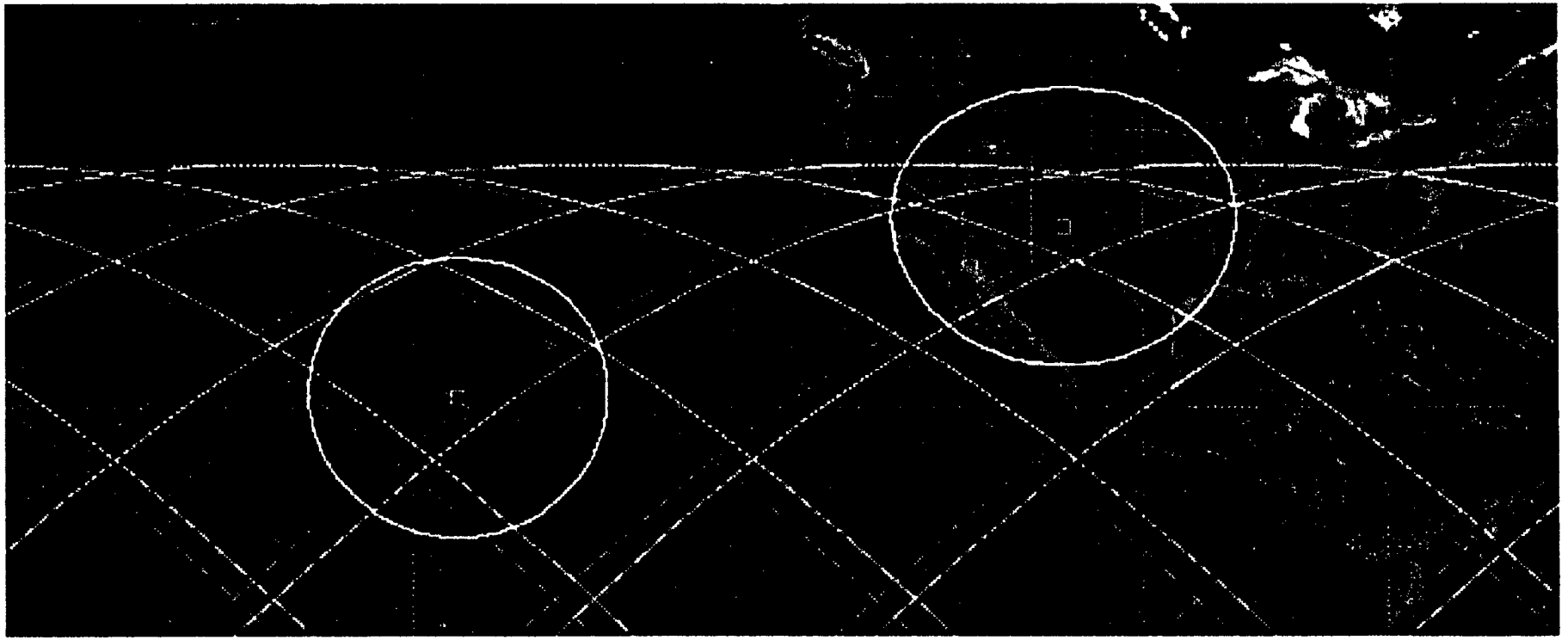

If satellite altitude is at least 600 km, only a phase change is required to enable SOR-Maui link

- Altitude: 1000 km
- Inclination: 40°
- Satellite separation: 45°
  - ~ 5600 km

Schafer

SOR to Maui 2-Bounce Relay
Link Availability

- Results of 1-year simulation (1-minute time steps)
  - Link availability (not including PCFLOS)
    - » Number of valid links per year: 570
    - » Average link is open 5.4 minutes
- Relay mirror design drivers
  - Maximum uplink: 1702 km
  - Maximum crosslink: 5647 km
  - Maximum downlink: 1702 km
  - Maximum total range: 9043 km
  - Minimum beam turning angle: 22.6°
    - » Average: 72 °
  - Maximum slew rate: 365 μrad / sec

Schafer

Link Efficiency
SOR 2-bounce relay to Maui

Transmitter diameter = 3.5 m
λ = 1 μm
Uniform illumination of xmtr aperture
No jitter or wavefront error

Transmitter optics transmission = 0.6
Bifocal optical transmission = 0.8
Atmospheric transmission each way: 0.8

Transmitter focused at first relay mirror, which is focused at second relay mirror
Second relay mirror focused at target

- Results for 1300-km up and downlink; 5600-km crosslink
  - Fraction of transmitted pulse energy inside 1-meter spot at target
    - » 1.0-meter relay mirror: 0.0013
    - » 1.5-meter relay mirror: 0.0045
  - Energy per pulse required at transmitter to put 100 mJ on target
    - » 1.0-meter relay mirror: 77 J
    - » 1.5-meter relay mirror: 22 J

Schafer

Imaging Considerations

Example imagery from EarthWatch web site

(actual image)

.5-m resolution

(actual image)

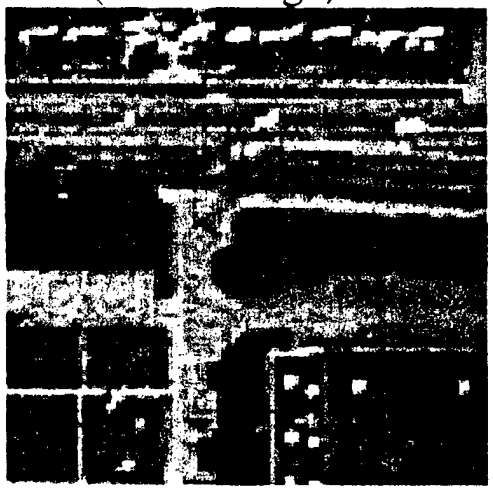

1-m resolution

(simulated image)

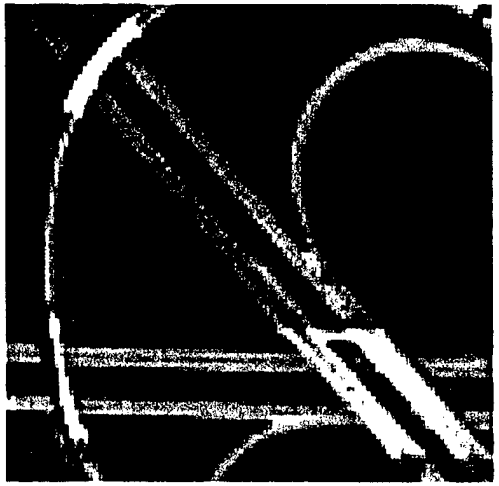

3-m resolution

Imaging aperture diameter	.5-m resolution	1-m resolution	3-m resolution
1 m	820 km	1600 km	4900 km
1.5 m	1200 km	2500 km	7400 km

(Range at which Rayleigh criterion is met at 0.5 μm)

Schafer

Synthetic Color Images with 1.5m Aperture
Camouflaged Scud Launcher Against Desert Background

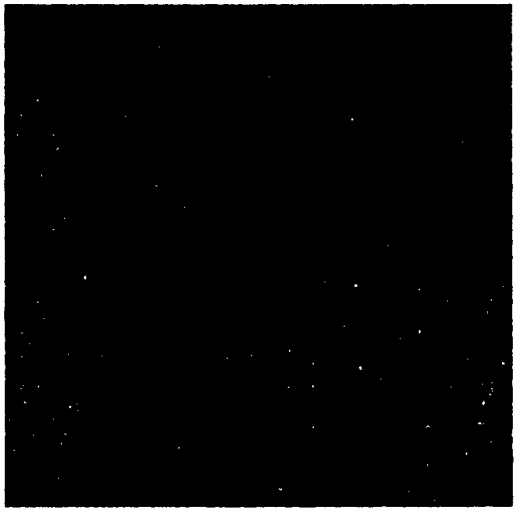

(truth) .25 m/pix

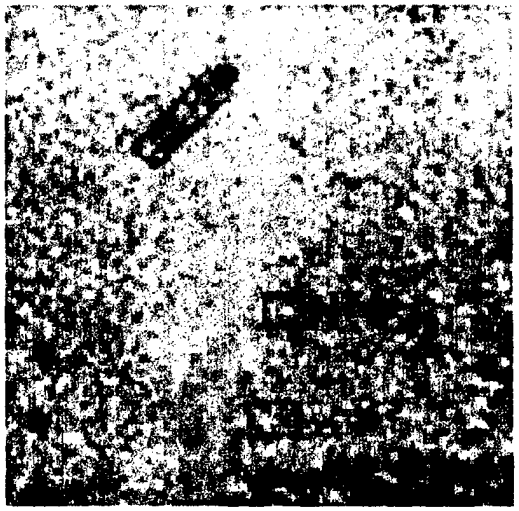

500 km .18m/pix

1000 km .37m/pix

1500 km .55m/pix

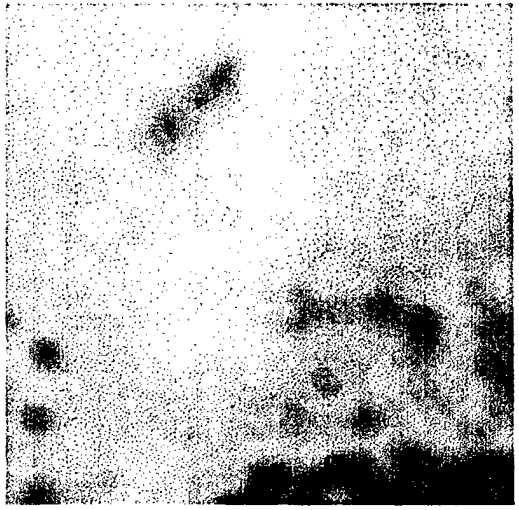

2000 km .73m/pix

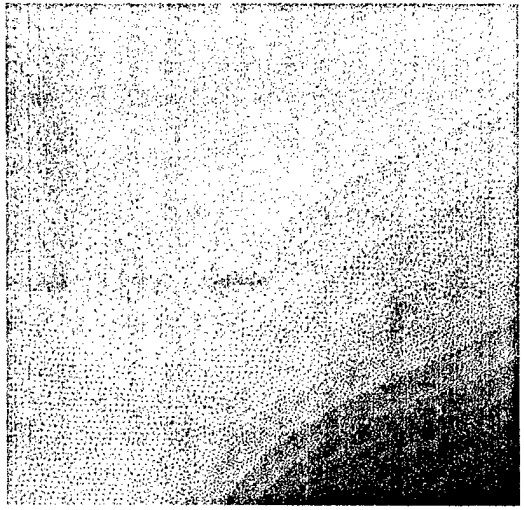

20,000 km 7.33 m/pix

Schafer

Required Future Work

- Modeling of jitter and wavefront error
  - Jitter: convolve Gaussian function with diffraction patterns
  - Wavefront: add random residual phase error to aperture function
- Modeling of sensor / receiver systems
  - Target identification system
  - Laser target designator
  - Doppler wind measurement
- Modeling of pointing, acquisition, and tracking
- Analysis of multi-wavelength operations
  - Thermal issues at mid- to long-IR

Backup slides follow

Schafer

Throughput (Diffraction Only)

Range units: Mm
Diameter units: m

$I_{Pk}R^2_{Tgt}/D^2_{RM}$

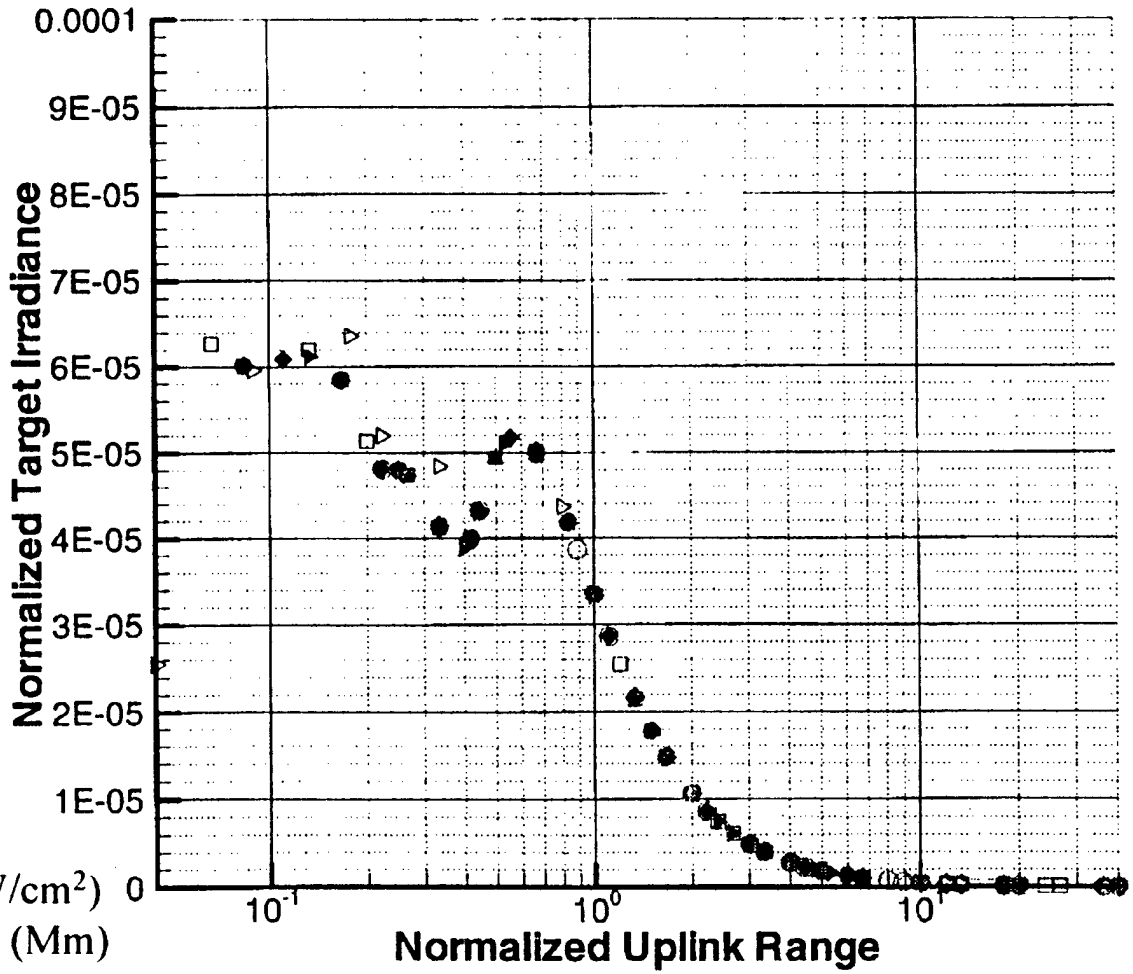

$R_u/(D_{Tx}D_{RM})$

I_{Pk} = peak intensity at target (W/cm^2)
R_{Tgt} = range from RM to target (Mm)
D_{RM} = diameter of RM (both apertures) (m)
R_u = uplink range (Mm)
D_{Tx} = diameter of ground transmitter (m)

Source: John Erkkila, Logicon RDA